SYMCOMP 2015
Faro, March 26-27, 2015

AN OVERVIEW ON THE MULTIDIMENSIONAL OPTIMAL ORDER DETECTION METHOD

Stéphane Clain[1,2], Jorge Figueiredo[1], Raphael Loubère[2], Steven Diot[2]

1: Centre of Mathematics
School of Sciences
University of Minho
Campus de Azurém, 4800-058 Guimarães, Portugal
e-mail: clain@math.uminho.pt

2: Institut de Mathématiques de Toulouse
Université Paul Sabatier
31062 Toulouse, France

Keywords: finite volume, polynomial reconstruction, hyperbolic problem, MOOD

Abstract. *Finite volume method is the usual framework to deal with numerical approximations for hyperbolic systems such as Shallow-Water or Euler equations due to its natural built-in conservation property. Since the first-order method produces too much numerical diffusion, popular second-order techniques, based on the MUSCL methodology, have been widely developed in the '80s to provide both accurate solutions and robust schemes, avoiding non-physical oscillations in the vicinity of the discontinuities. Although second-order schemes are accurate enough for the major industrial applications, they still generate too much numerical diffusion for particular situations (acoustic, aeronautic, long time simulation for Tsunami) and very high-order methods i.e. larger than third-order, are required to provide an excellent approximation for local smooth solution as well as an efficient control on the spurious oscillations deriving from the Gibbs' phenomenon. During the '90s and up to nowadays, two main techniques have been developed to tackle the accuracy issue. The ENO/WENO which can cast in the finite volume context mainly concerns structured grids since the unstructured case turns to be very complex with a huge computational cost. The Discontinuous Galerkin method handles very well accurate approximations but the computational cost and implementation effort are also very high. In 2010 was published a seminal paper that proposed a radically different method. The philosophy consists to use an a posteriori approach to prevent from creating oscillations whereas the traditional methods employ an a priori method which dramatically cuts the accuracy order. In this document, I shall briefly present the MOOD method, show its main advantages and give an overview of the current applications.*

1 A SMALL HISTORICAL INTRODUCTION

Numerical schemes for hyperbolic problems date back from the beginning of the '50s with the *Mathematical And Numerical Integrator And Calculator* Project (MANIAC project) to calculate the nuke fission or solve simple hydrodynamic problems [1, 2]. Finite difference was the unique framework to design numerical schemes and reaches the peak of its golden age with the book of Richtmyer and Morton [3]. Nevertheless, the method suffers of two major drawbacks: it is not conservative and continuity of the solution is required (at least) since one has to define punctual real values at the grid nodes. In a pioneer work, S. K. Godunov proposes in 1959 [4] a new method based on flux evaluations across the interfaces between cells. The main benefits are the built-in conservation property and the use of the mean values which enable discontinuous solutions discretization. The method takes advantage of the divergence form of the conservation laws and makes use of the divergence theorem (or Green theorem) on each cell, providing a set of semi-discrete equations associated to the constant piecewise unknowns. Such a method is very robust but suffers of a large amount of numerical diffusion providing at most a first-order scheme. Linear second-order methods such as the Lax-Wendroff method, *i.e.* the coefficients combining the unknown values do not depend on the solution, suit very well for smooth solutions but the so-called Gibbs' phenomenon occurs when dealing with discontinuities: oscillations characterized by local overshoots and undershoots create non physical approximations and should be eliminated. In the '70s, Van leer [5] introduces an important new concept: the Monotonic Upstream-Centered Scheme for Conservation Laws method (or MUSCL method) where a non-linear procedure is applied to eliminate the creation of new extrema still preserving a local linear representation in the smooth regions of the solution. Extensions for non-linear hyperbolic problems for two- or three-dimensional geometries give rise to a very important literature up to nowadays [6] and the technique is still very popular in the industrial context (most of the hydrodynamics codes use the MUSCL limiter) while almost all finite volume commercial codes implement the technique. The main drawbacks of the MUSCL method are its limitation to second-order schemes (with some rare exceptions) and the procedure strongly reduces the optimal accuracy. To provide higher order, a new method was proposed in the '90s based on the selection of several polynomial reconstructions associated to a given cell[7] such that, on the one hand, the accuracy is optimal for smooth solution and, on the other hand, the method reduces the creation of oscillations controlled by a smoothness indicator. The Essentially Not Oscillating method (ENO) and its Weighted version WENO were the state of the art of the very high-order (larger than three) finite volume methods at the beginning of the 2010s and the reader can refer to the recent review in [8]. In 2010, we have initiated a series of papers on the development of a new technology to suppress the oscillations while preserving the high accuracy for the smooth solutions. The Multidimensional Optimal Order Detection method radically differs from the other techniques since it is based on an *a posteriori* approach (or objective approach) whereas the traditional way addresses an

a priori procedure (or speculative approach) to determine whether or not a polynomial reconstruction is eligible. Moreover, unlike to the other methods, we can plug some physical constraints into the limiting (detection) procedures which turns out a very good advantage with respect to the traditional methods.
The rest of the paper is as following. We give the general framework of the finite volume method using very high-order approximations for hyperbolic systems. We address a short issue on the polynomial reconstructions and highlight the major difficulties to provide the optimal accuracy. Section three is dedicated to the MOOD method where we detail the algorithm and highlight the main advantages with respect to the traditional methods. We give in the fourth section some examples of numerical applications where we assess the accuracy and demonstrate the robustness of the method.

2 VERY HIGHT-ORDER FINITE VOLUME METHOD

For the sake of simplicity, we shall consider a hyperbolic scalar problem on a bounded domain Ω where one seek the function $\phi \stackrel{\Delta}{=} \phi(t,x)$ such as

$$\partial_t \phi + \partial_{x_1} F_1(\phi) + \partial_{x_2} F_2(\phi) = 0 \tag{1}$$

where $F_1(\phi)$ and $F_2(\phi)$ are the physical flux with $x = (x_1, x_2)$. We prescribe the Dirichlet condition $\phi = \phi_D$ on the inflow interface Γ^- given by

$$\Gamma^- = \{x \in \partial\Omega;\ F_1'(\phi_D)n_1 + F_2'(\phi_D)n_2 < 0\}, \quad \Gamma^+ = \{x \in \partial\Omega;\ F_1'(\phi_D)n_1 + F_2'(\phi_D)n_2 \geq 0\},$$

with $n = (n_1, n_2)$ the outward normal vector on the boundary while F_1' and F_2' stands for the derivatives of the physical flux with respect to ϕ. As an example, the linear convection equation $F_1(\phi) = u_1\phi$ $F_2(\phi) = u_2\phi$ cast in the general framework. Shallow water equations or the Euler system cast in a more general vector-values hyperbolic system where the boundary conditions turns to be more complex to be defined.

2.1 Mesh and notations

We introduce the following notations illustrated in Figure 1 to design the numerical scheme. The computational domain Ω is assumed to be a polygonal bounded set of $\mathbb{R}^2$ divided into polygonal cells c_i with m_i the cell centroid, $i \in \mathcal{E}_{el}$ the cell index set. For a given cell c_i, we denote by e_{ij} the edges of c_i such that

- $j \in \mathcal{E}_{el}$ if there exists an adjacent cell c_j with $e_{ij} = c_i \cap c_j$;
- $j = D$ if $e_{iD} = c_i \cap \Gamma_D$.

To avoid a specific treatment of the boundary edges we introduce $\widetilde{\mathcal{E}_{el}} = \mathcal{E}_{el} \cup \{D\}$, the cell index set augmented with index D for the Dirichlet condition and N for the reflection/transmission condition. We then define the set ν_i of all the indexes $j \in \widetilde{\mathcal{E}_{el}}$ such that

e_{ij} is an edge of c_i.
For each edge e_{ij}, $i \in \mathcal{E}_{el}$, $j \in \nu_i$, n_{ij} stands for the unit normal vector going from c_i to c_j and τ_{ij} is the unit tangent vector such that n_{ij}, τ_{ij} is a counter-clockwise oriented basis. We denote by m_{ij} the edge midpoint, while $\big(\xi_r, q_{ij,r}\big)$, $r = 1, ..., R$ stands for the quadrature rule for the numerical integration on e_{ij}, where ξ_r is the weight associated to the r^{th} quadrature point $q_{ij,r}$. If index $j = D$ (resp. $j = N$), n_{iD} and τ_{iD} represent the outward unit normal vector and unit tangent vector while m_{iD} and $q_{iD,r}$ are the edge midpoint and Gauss points.

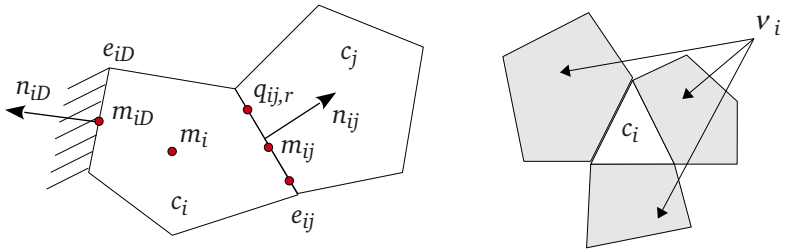

Figure 1: Mesh and notations (left). Definition of index set ν_i (right).

The generic first-order finite volume scheme writes

$$\phi_i^{n+1} = \phi_i^n - \Delta t \sum_{j \in \nu_i} \frac{|e_{ij}|}{|c_i|} \mathcal{F}_{ij}^n, \tag{2}$$

where ϕ_i^n is an approximation of the mean value of V at time t^n on cell c_i, Δt stands for the time step, $|e_{ij}|$ and $|c_i|$ are, respectively, the length of edge e_{ij} and the area of cell c_i. Vector $\mathcal{F}_{ij}$ represents a numerical approximation of the conservative flux across the interface e_{ij}. In the following, we shall denote by Φ the vector collecting all the approximation ϕ_i^n, $i \in \mathcal{E}_{el}$.

2.2 Polynomial reconstructions

To improve the accuracy of the scheme, polynomial reconstruction are providing in order to evaluate a very good approximation on both side of the interface we shall plug into the numerical flux. To achieve high-order approximations, polynomial reconstructions are involved to produce local representations of the approximation (see [9, 10, 12] for the conservative case and [13] for the extension to the diffusive flux case). We recall here the

fundamental lines of the reconstruction for the sake of consistency and to introduce the notations.
For a given cell c_i and a polynomial degree d, we associate the stencil $S(c_i, d)$ constituted of cells we pick-up around the reference cell c_i and we shall denote by $\boldsymbol{\phi}_i(\mathbf{x}; d)$ a local polynomial function of degree d associated to cell c_i with the following structure

$$\boldsymbol{\phi}_i(\mathbf{x}; d) = \phi_i \ + \sum_{1\leq|\alpha|\leq d} \mathcal{R}_i^\alpha \Bigg((\mathbf{x} - m_i)^\alpha - M_i^\alpha \Bigg),$$

with ϕ_i an approximation of the ϕ mean value on cell c_i, $\alpha = (\alpha_1, \alpha_2)$ the multi-index, $|\alpha| = \alpha_1 + \alpha_2$ (see [12] for a detailed description) and

$$M_i^\alpha = \frac{1}{|c_i|} \int_{c_i} (\mathbf{x} - m_i)^\alpha \, d\mathbf{x},$$

such that the following conservativity property holds

$$\frac{1}{|c_i|} \int_{c_i} \boldsymbol{\phi}_i(\mathbf{x}; d) \, d\mathbf{x} = \phi_i.$$

To compute the reconstruction coefficients, we introduce the quadratic functional

$$E_i(\mathcal{R}_i) = \sum_{\ell \in S(c_i,d)} \left(\frac{1}{|c_\ell|} \int_{c_\ell} \boldsymbol{\phi}_i(\mathbf{x}; d) \, d\mathbf{x} - \phi_\ell \right)^2,$$

where ϕ_ℓ are approximated mean values on cells c_ℓ of the stencil and $\mathcal{R}_i = (\mathcal{R}_i^\alpha)_{1\leq|\alpha|\leq d}$ is the vector which gathers all the components. We seek for vector $\mathcal{R}_i$ which minimises the functional and denote by $\widehat{\phi}_i(\mathbf{x}; d)$ the associated polynomial. In [13], a detailed presentation of the method is given to provide the solution $\mathcal{R}_i$. An important point is the consistancy of the reconstruction process with all the polynomial of degree d to guarantee that we achieve a $d+1$th-order of accuracy.

2.3 The generic finite volume scheme

Numerical flux $\mathcal{F}_{ij}^n$ in relation (2) is a first-order of approximation of the exact mean value of the flux across the interface

$$\frac{1}{|e_{ij}|} \int_{e_{ij}} \big(F_1(\phi(t,x))n_1 + F_2(\phi(x,t))n_2 \big) ds.$$

To provide a better approximation of the flux, one has to first use a high order quadrature rule for the flux integration along the edge using Gauss points $q_{ij,r}$, and secondly, an

accurate approximation at the Gauss points. Then the generic high order finite volume scheme writes

$$\phi_i^{n+1} = \phi_i^n - \Delta t \sum_{j \in \nu_i} \frac{|e_{ij}|}{|c_i|} \sum_{r=1}^{R} \xi_r \mathbb{F}(\widehat{\phi}_i(q_{ij,r}; d), \widehat{\phi}_j(q_{ij,r}; d), n_{ij}), \tag{3}$$

with ξ_r the weights of the quadrature formulae and $\mathbb{F}(\cdot, \cdot, n_{ij})$ the numerical flux from c_i toward c_j. For example the upwind flux or the Lax friedrichs flux are commonly used in the case of the advection but other flux are proposedin [14].

3 THE MOOD METHOD

Relation (3) coupling with the polynomial reconstruction and assuming that Δ satisfies some stability CFL condition provides a very accurate approximation when dealing with smooth solution. unfortunately, it is well-known that even with smooth initial and boundary condition, solutions may present discontinuities and the stability no longer holds while non physical oscillations give rise. The main goal is to locally reduce the polynomial degree in domains where the solution is discontinuous while preserving the optimal order where the function is smooth.

3.1 The *a priori* limiting procedure versus the *a posteriori* detection

Limiters are non-linear procedures providing a reduction of the polynomial degrees to reinforce the stability. We refer to *a priori* limiting procedures in relation with the update step *i.e.* the stage which consists in assembling the flux contributions of each interface of the cell. Therefore, an *a priori* limiting procedure modifies the polynomial function used to evaluate $\widehat{\phi}_i(q_{ij,r}; d)$ and $\widehat{\phi}_j(q_{ij,r}; d)$.
As an example, the MUSCL technique is base on a local linear reconstruction $\widehat{\phi}_i(\mathbf{x}; 1) = \phi_i + \mathbf{a_i}(\mathbf{x} - m_i)$ where $\mathbf{a_i}$ stands for a first-order approximation of the gradient. To annihilate the Gibbs' effect, a limiter $\chi_i \in [0, 1]$ is introduced into the reconstruction and we set $\widehat{\phi}_i(\mathbf{x}; 1) = \phi_i + \chi_i \mathbf{a_i}(\mathbf{x} - m_i)$ such that $\chi_1 = 0$ provides the first-order scheme. The value of the limiter is obtained via an local analysis of the gradient in the vicinity of the cells. We sum-up the main drawback of the limiting procedure.

- No physical considerations are introduced in the computation of χ_i such as the positivity preserving principle.
- The limiter is almost activated even when not necessary. This is the main problem of the *a priori* procedure since it is based on the "precautionary principle" leading to an over-limitation which results into a strong reduction of accuracy.
- The *a priori* procedure is always carried out for each cell since is no simple way to detect if the limiting algorithm is really necessary. Unnecessary computational overheads result from this consideration.

- Mathematical properties such as the maximum principle are hard to achieved with second-order scheme and the CFL condition is usually more restrictive inducing more time steps to compute.

In other words, the *a priori* philosophy is blind and operates indiscriminately without indications on the real requirements and consequences on the updated approximations. The MOOD method is based on an *a posteriori* philosophy where, in short, the idea consists in using the maximum polynomial degree for the reconstruction, to evaluate the flux, to update the solution and then make some corrections only if it is really necessary, up to the user criteria. The main advantage is that we have new and objective informations deriving from a predictor called the candidate solution that we analyse and check to determine which cells or polynomial functions have to be really modified. The *a posteriori* concept enables to dramatically reduce the computational cost, integrate physical properties and better preserve the accuracy.

3.2 The MOOD loop

The main idea of the MOOD method is to determine, for each cell, the optimal degree that one can employ in the polynomial reconstruction that provides both the best accuracy and satisfies some stability conditions. In the following, we summarise the main ingredients of the method and refer to [10, 12] and the reader can find some extension in [15, 16, 17, 18]. The point is to compute an admissible and accurate solution Φ^{n+1} from Φ^n in a sense we shall present is the sequel. To this end, we introduce the Cell Polynomial Degree d_i (in short CellPD) as the degree of the polynomial function associated to cell c_i, while d_{ij} stands for the Edge Polynomial Degree (in short EdgePD) associated to edge e_{ij}. We deduce the EdgePD map from the CellPD map using the simple rule $\mathsf{d}_{ij}=\min(\mathsf{d}_i,\mathsf{d}_j)$ and compute the approximations $\phi_{ij,r}$, $\phi_{ji,r}$, $r=1,\ldots,R$ at point $q_{ij,r}$ on both sides of the edge using the polynomial reconstructions $\widehat{\phi}_i$ and $\widehat{\phi}_j$ of degree d_{ij}. The main problem is the determination of the CellPD map such that the solution $(Phi)^{n+1}$ is admissible. A fundamental assumption underlying the method is that the first-order scheme (also named the parachute scheme) will satisfy all the requirements of what we shall call an eligible solution. Consequently, one can reduce the polynomial degree until reaching the first-order scheme if necessary in the worst cases and then provide an admissible approximation. Parachute scheme are the usual upwind, Rusanov, HLL schemes which have very good properties from the stability point of view but generate a large amount of numerical diffusion.
Two independent mechanisms are involved in the MOOD method: the detection procedure and the limitation procedure. The detection stage is based on the notion of $\mathcal{A}$-eligible set, where we check each cell to determine whether the numerical solution is admissible or not. The limitation procedure mainly consists in reducing the polynomial degree where it is necessary to avoid the appearance of numerical instabilities.

3.2.1 $\mathcal{A}$-eligible set

The detection procedure is the core of the method. We establish criteria to determine whether the approximation of the mean values on cells correspond to an admissible solution or not. We here rephrase the abstract framework proposed in [10, 12] and denote by $\mathcal{A}$ the set of detection criteria (for example the positivity of the water height in the shallow-water context) that the numerical approximation has to respect on each cell. We say that a candidate solution is $\mathcal{A}$-eligible if it fulfils all the criteria of $\mathcal{A}$.
If the candidate solution is not $\mathcal{A}$-eligible on cell c_i, then we reduce the polynomial degree of the respective cell. However, the solution may not be $\mathcal{A}$-eligible regardless of the set $\mathcal{A}$ even if the polynomial degree is zero for the cell. Consequently, we shall consider the numerical solution *acceptable* on the cell if either it is $\mathcal{A}$-eligible or is a first-order approximation (*i.e.* the CellPD has been decremented to zero). Several techniques have been developed in [10, 12] to reduce the computational cost and avoid re-evaluation of all the fluxes on the whole domain. On the other hand, we extend the MOOD algorithm initially designed for a one-time step Euler scheme to the TVD-RK3 scheme by applying the MOOD procedure to each sub step of the TVD-RK3 procedure. Therefore, for sake of simplicity, in the following we shall present the MOOD procedure for just one step, bearing in mind that the TVD-RK3 scheme is a succession of sub steps. Other methods to compute the candidate solution in time use the ADER methodology.We refer to [18] for a presentation of the MOOD procedure in that case.

3.2.2 Candidate Solution and evaluation

In Figure 3.2.2, we display the principle of the MOOD loop. Assume that an approximation Φ^n is known. We first set the CellPD at the maximum polynomial degree value such that we carry out the reconstruction with the highest accuracy. We plug the values at the Gauss points into the numerical flux and then evaluate the candidate solution $\Phi^\star$. Each cell are analysed to check whether it is eligible or not. The problematic cells are then corrected by the reduction of the polynomial degree and new polynomial reconstructions, new flux are evaluated, providing a new candidate solution .

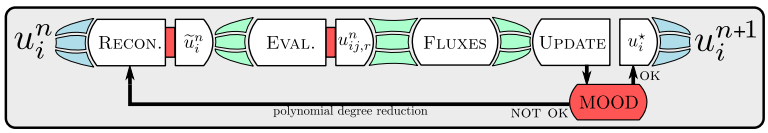

Figure 2: The MOOD loop

The loop stops when all the cell pass all the criteria of the $\mathcal{A}$-eligible set. Then the candidate solution $\Phi^\star$ turns to be the solution Φ^{n+1} at time t^{n+1}. It is important to notice

that only the interface which the cells have been modified have to be recomputed hence the computational cost associated to a re-evaluation of the cell is very low.

3.2.3 Detection criteria and detector chain

A detector is a criterion which enable to quantify or qualify the local candidate solution. From the detector, one can take a decision about the eligibility of the cell. Usually, several detectors are involved in a so-call detector chain where each detector evaluate a specific aspect of the solution such as the positivity, the smoothness, the oscillations and so on. Some detectors notice that the cell is or may potentially be problematic while other detectors release the potential problematic cells. We report to [11] and [19] for a list of detectors.
To highlight the method, we just present two simple detectors. The Physical Admissible Detector (PAD) requires that the candidate solution $\phi_i^\star > 0$ and is very important for the shallow water problem $\phi = h$ the water height or for the Euler system $\phi = \rho$. An other PAD could be $\phi_i^\star \in [0, 1]$ which is very important if we are dealing with a mass or a volume fraction. A second detector is the Extrema Detector (ED) which check if $\phi_i^\star$ is a local extremum with respect to the neighbour cells. Indeed, when an oscillations is created, new extrema are generated and the (ED) detects potential over- or under-shoots. The detector chain organization is very important to safe computational resource and take very quickly a decision. For example if we detect that the solution is negative with the PAD, we immediately state that the cell is problematic and no more evaluation for this cell is required. In the same way, if the (ED) is not activated (we do not have an extremum), we immediately mark the cell as clean and no more effort are necessary.It result that only a very small number of cells are really treated (less than 5% in practice) hence the detection procedure is very fast. Moreover, one can easily check that the detection procedure is highly parallelizable since the analysis of each cell is independent from one to each other. An other interesting point is that the choice of the variables used for the detection process may be different from the primitive or conservative ones. For instance, in [15] the entropy is used in the detector to keep the scheme from violating the entropy condition.

4 NUMERICAL TESTS AND EXAMPLES

We present several test cases where the efficiency, robustness and accuracy of the MOOD method are highlighted. Numerical errors are evaluated in the L^1 and L^∞ norms setting

$$L^1\text{-error:} \quad \sum_{i=1}^{I} |\phi_i^N - \phi_i^{ex}|/I \quad \text{and} \quad L^\infty\text{-error:} \quad \max_i |\phi_i^N - \phi_i^{ex}|,$$

where (ϕ_i^{ex}) and (ϕ_i^N) are respectively the exact and the approximated mean values of function ϕ on cell c_i at the final time $t^N = T$ and $I = \#\mathcal{E}_{el}$.

4.1 Linear convection

We first consider the simple convection of the double sine function on the academic square with periodic condition given by

$$\partial_t \phi + \nabla.((1,1)^t \phi) = 0$$

where the initial function is $\phi(0,x) = \sin(2\pi x_1)\sin(2\pi x_2)$. Figure 3 presents the convergence rate using two different detector chains. The first one (left panel) only detect the extrema and set the CellPD to 0 whether the extremum derives from an oscillation or is a real and smooth extremum. The second detector chain is supplemented with a smooth detector which release the (ED) when dealing with a smooth extrema. It results that the second chain enable the optimal error for all the reconstruction considered in the simulation.

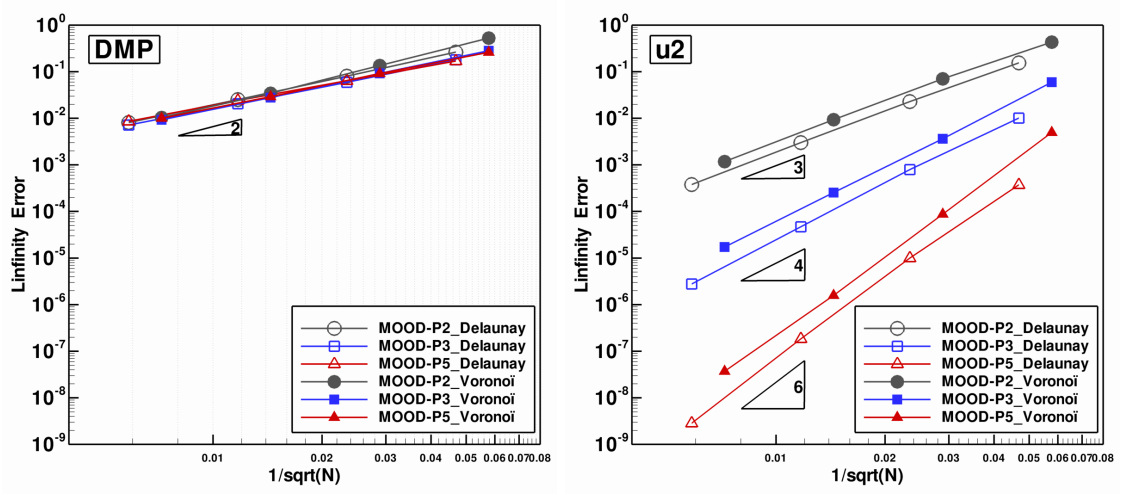

Figure 3: Advection of the double sine function with a constant velocity and periodic condition. Convergence curves with different detectors.

An other classical test is the slotted cylinder problem. The velocity is not constant but define a global rotation with respect to the origin. After a full revolution, Figure 4 left top panel gives an general view of the three shapes that rotate while the top central panel zooms out the slotted cylinder. After a full revolution, the slotted cylinder is smeared and the gap has almost disappeared when using the traditional MUSCL method as presented in the right top panel. The $\mathbb{P}_1$ reconstruction associated to the MOOD method provides a lightly better results (bottom left panel) but the $\mathbb{P}_3$ and $\mathbb{P}_5$ reconstructions manage to preserve the shape. Notice that after half of revolution, the cylinder crosses a portion of the mesh where the cells size are of the same order of the gap. In all the simulations, the maximum principle is strictly respected and no over- or under-shoots are reported.

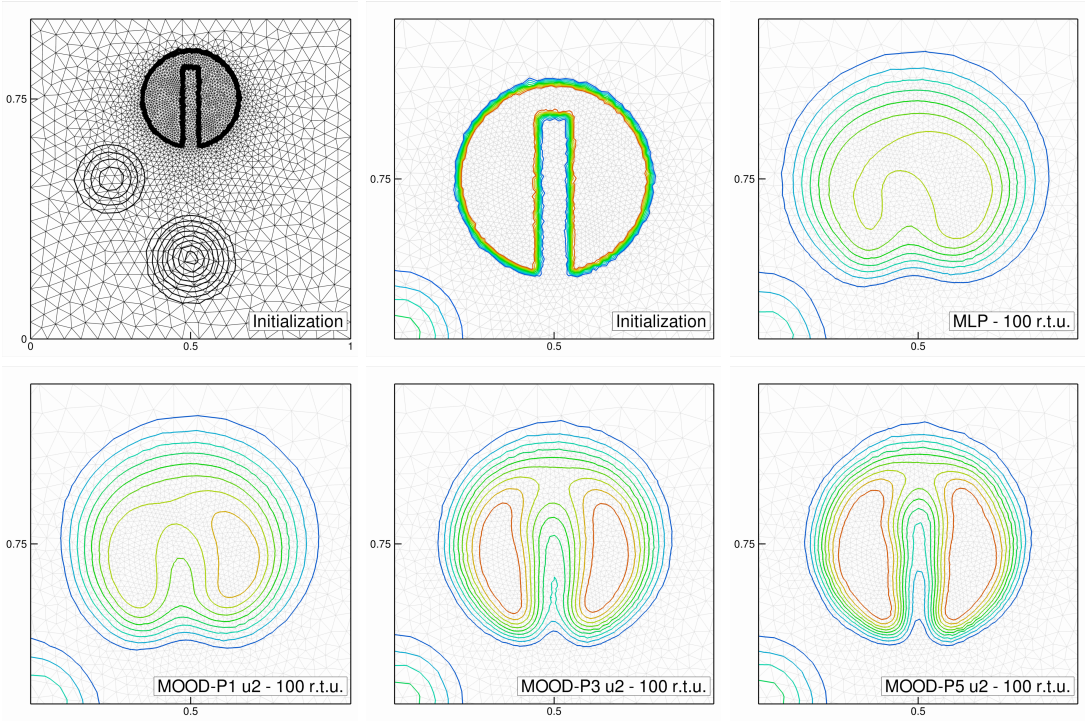

Figure 4: Full revolution of several geometrical figures. The slotted cylinder is well-preserved when using very high-order reconstruction. No maximum principle violation are reported in the simulations.

4.2 Shallow water equations

The shallow water is an important applications for the modelling of river, coast or Tsunami. In [11], the shallow-water system equipped with the non-conservative term deriving from the varying bathymetry is considered

$$\begin{aligned}
&\partial_t h + \nabla.(hU) = 0,\\
&\partial_t (hU) + \nabla.(hU \otimes U + \frac{1}{2} g h^2 I_2) = -gh\nabla b,
\end{aligned}$$

where h is the water height, $U = (u_1, u_2)^T$ the velocity, $U \otimes U$ the tensorial product, $Q = hU$ the mass flow, I_2 the $\mathbb{R}^2$ identity matrix, b the bathymetry with respect to a reference level and g the gravitational acceleration. A sophisticated finite volume method using the MOOD methodology was used to provide numerical approximations.
a steady-state vortex flow with varying bathymetry characterised by

$$H(x,y) = H_\infty - \frac{A^2}{4g} e^{2(1-r^2)}, \quad u(x,y) = A\hat{y}e^{(1-r^2)}, \quad v(x,y) = A\hat{x}e^{(1-r^2)},$$

with $\hat{x} = x - x_0$, $\hat{y} = y - y_0$, and $r^2 = \hat{x}^2 + \hat{y}^2$. We take $H_\infty = 1$, $A = 1$, and $x_0 = y_0 = 0$, while the bathymetry function is given by $b(r) = 0.2e^{(1-r^2)/2}$. Figure 5 depicts the geometry of the vortex as well as the velocity field for the square domain $\Omega = [-3, 3] \times [-3, 3]$.
The simulations are carried out until the final time $t_{\text{final}} = 1\,s$ where we test the MOOD procedure performance using different detectors, namely the DMP against DMP+u2. For that purpose, we consider four Delaunay meshes of 800, 3194, 12742 and 50958 triangles and perform simulations with $\mathbb{P}_2$, $\mathbb{P}_3$ and $\mathbb{P}_5$ for the conservative variables, while the reconstruction for the b function is exact with the $\mathbb{P}_2$ polynomial. Initial conditions are prescribed using the steady-state solution and the Dirichlet boundary conditions imposed on the Gauss points of the boundary edges. The convergence results obtained for the total height are presented in Table 1.

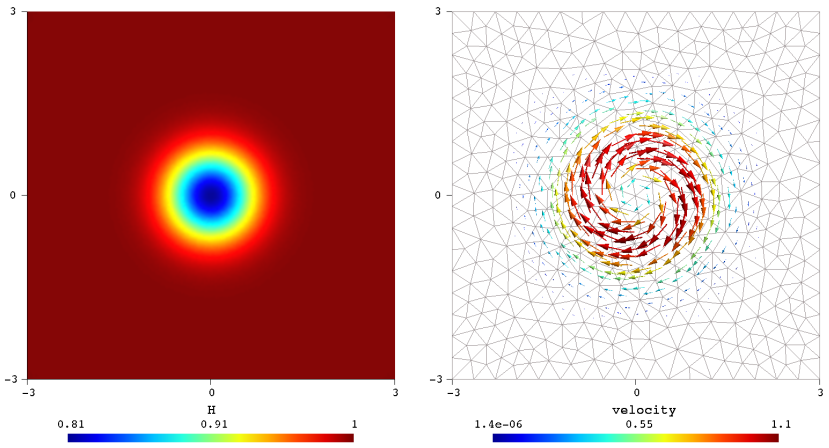

Figure 5: Free surface and velocity field for the static vortex with a 800 triangles mesh.

We report that we obtain the optimal order in all the cases and highlight the capacity of the MOOD method to deal with non-conservative problem.

Table 1: Total height L^1- and L^∞-errors and convergence order for the static vortex.

Nb of Cells	$\mathbb{P}_2$				$\mathbb{P}_3$				$\mathbb{P}_5$			
	err_1		err_∞		err_1		err_∞		err_1		err_∞	
800	4.85e-04	—	6.82e-03	—	8.69e-05	—	1.39e-03	—	3.89e-05	—	9.25e-04	—
3194	7.66e-05	2.7	9.99e-04	2.8	5.86e-06	3.9	8.16e-05	4.1	6.64e-07	5.9	1.41e-05	6.0
12742	1.02e-05	2.9	1.41e-04	2.8	3.67e-07	4.0	5.57e-06	3.9	1.05e-08	6.0	2.21e-07	6.0
50918	1.30e-06	3.0	1.86e-05	2.9	2.29e-08	4.0	4.26e-07	3.7	1.82e-10	5.9	3.55e-09	6.0

A more complex and realistic simulation test is an extension of the classical 2D partial

dam-break problem (see *e.g.* [20] and references therein). We assume that the reservoir (left part of the domain in Figure 6) is higher than the river (right part of the domain), the two entities being relied by a ramp with constant slope. We study the outflow just after the dam rupture until a final simulation time $t_{\text{final}} = 7\,s$. Several characteristic structures will be analysed to evaluate the scheme accuracy and robustness, namely numerical diffusion of the discontinuity, the vortexes deepness as an accuracy assessment and the oscillations around shocks generated by the outflow as a robustness assessment. The domain we

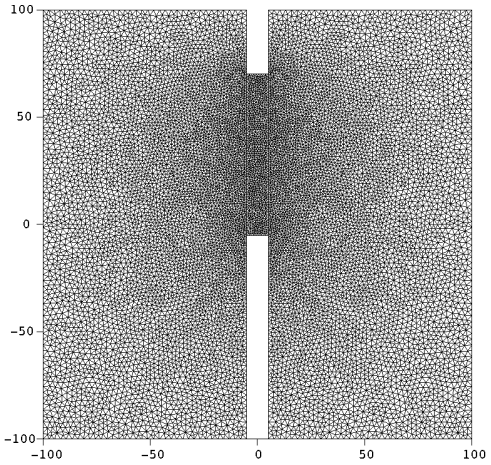

Figure 6: Partial dam-break geometry and the Delaunay mesh (24750 triangles).

consider has been proposed in [20] and the Delaunay mesh, composed of 24750 triangles, is depicted in Figure 6. The breach corresponds to the sub domain $[-5, 5] \times [-5, 70]$ and the bathymetry function is given by

$$b(x,y) = \begin{cases} 1 & , \quad -100 \leq x < -5, \\ 0.1(5-x) & , \quad -5 \leq x < 5, \\ 0 & , \quad 5 \leq x \leq 100, \end{cases}$$

while the initial free surface is given by

$$H(x,y,0) = \begin{cases} 10 & , \quad -100 \leq x < 5, \\ 5 & , \quad 5 \leq x \leq 100. \end{cases}$$

At the initial time $t = 0$ the system is assumed to be at rest and we prescribe reflection boundary conditions on the whole boundary. The bathymetry is characterised by a $\mathbb{P}_1$ polynomial reconstruction since the domain is flat or constituted of a linear ramp. Numerical simulations have been carried out a chain of detectors which include the PAD, the Extrema Detector and the u2 detector (see [10]) which evaluate the smoothness of the

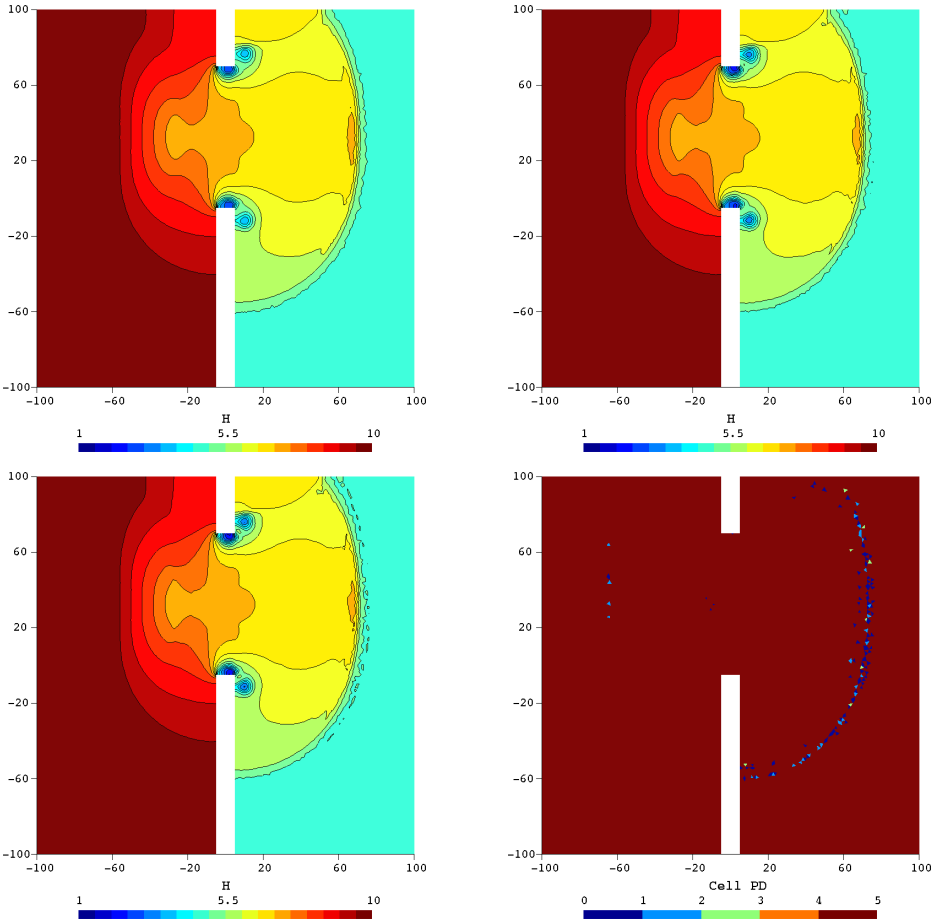

Figure 7: Total height at t_{final} using the DMP+u2$^{\nu}$ detector. Left top panel: $\mathbb{P}_2$. Right top panel: $\mathbb{P}_3$. Left bottom panel: $\mathbb{P}_5$. Right bottom panel: CellPD map with the $\mathbb{P}_5$ reconstruction at final time.

solution. we display in Figure 7 the total height at the final time using the new DMP+u2$^{\nu}$ detector for different polynomial reconstructions $\mathbb{P}_2$, $\mathbb{P}_3$ and $\mathbb{P}_5$. From the stability point of view, the oscillations nearby the shock wave are very well-contained for the $\mathbb{P}_2$ case and are small (below 0.6%) with the $\mathbb{P}_3$ reconstruction, mainly confined near the upper boundary. As for the $\mathbb{P}_5$ situation, oscillations are spread along a large part of the shock wave and represent up to 1.0% of the total height. The CellPD map (see Figure 7 right bottom) shows that the polynomial degree and we observe that in fact very few cells have to be cured.

4.3 Euler system

We end the series of numerical experiences with the Euler system which represents an excellent prototype of complex flow. We reproduce the equations

$$\partial_t \begin{pmatrix} \rho \\ \rho u_1 \\ \rho u_2 \\ E \end{pmatrix} + \partial_{x_1} \begin{pmatrix} \rho u_1 \\ \rho u_1^2 + p \\ \rho u_1 u_2 \\ u_1(E+p) \end{pmatrix} + \partial_{x_2} \begin{pmatrix} \rho u_2 \\ \rho u_1 u_2 \\ \rho u_2^2 + p \\ u_2(E+p) \end{pmatrix} = 0,$$

with ρ the density, $U = (u_1, u_2)$ the velocity, P the pressure, E the total energy per unit volume

$$E = \rho \left(\frac{1}{2}(u_1^2 + u_2^2) + e \right),$$

and we assume the equation of state $e = \frac{p}{\rho(\gamma - 1)}$.

We aim to reproduce the propagation of a shock in a cylinder and determine all the interactions and reflections between the waves and the wall. Figure 8 displays a picture of the cavity where an initial strong shock travelling from left to right hits the cavity and develops complex structures.

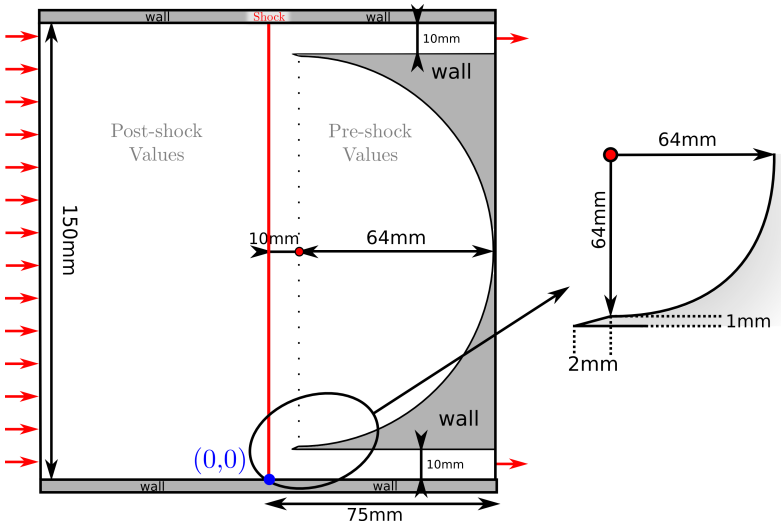

Figure 8: Design of the cavity. An incident pressure wave shocks with the curved cavity and generates complex reflection waves.

We give in Figure 9 the mesh used for the computation and underline that we mix different type of elements (triangle and quadrilateral cell) without any problem. Also notice that the mesh presents strong form factor that the reconstruction process and the MOOD method handle without any problem.

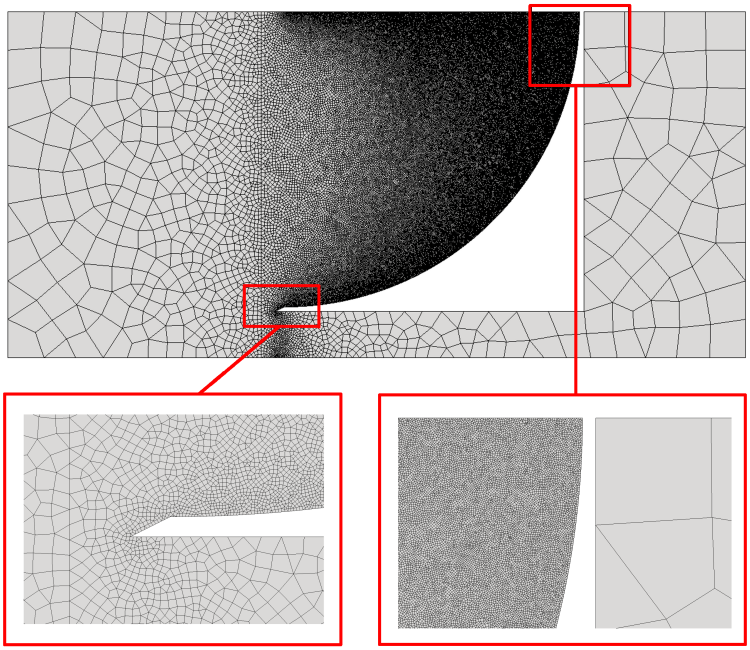

Figure 9: Mix 2D Mesh with 193.000 elements of the cavity

The simulations are carried out with the MOOD-P3 method (fourth-order) using the PAD and the u2 Detection Process. Figure 10 is rendered as a full mesh by symmetry even if the computation was done on a half-domain to easier compare with physical results of [21]. The simulation is clearly in agreement with the experience and demonstrate the high capacity of the MOOD method to handle complex shock structures and contact discontinuities.

5 CONCLUSIONS

In this document, we propose an overview of the MOOD method as a new technique to substitute the ENO/WENO or Discontinuous Galerkin framework. After five years of development, the methodology has grown up and becomes mature. In particular, the capacity to handle discontinuities, to track interfaces while preserving the accuracy for regular solutions have proved that the method turns to be an efficient alternative to the

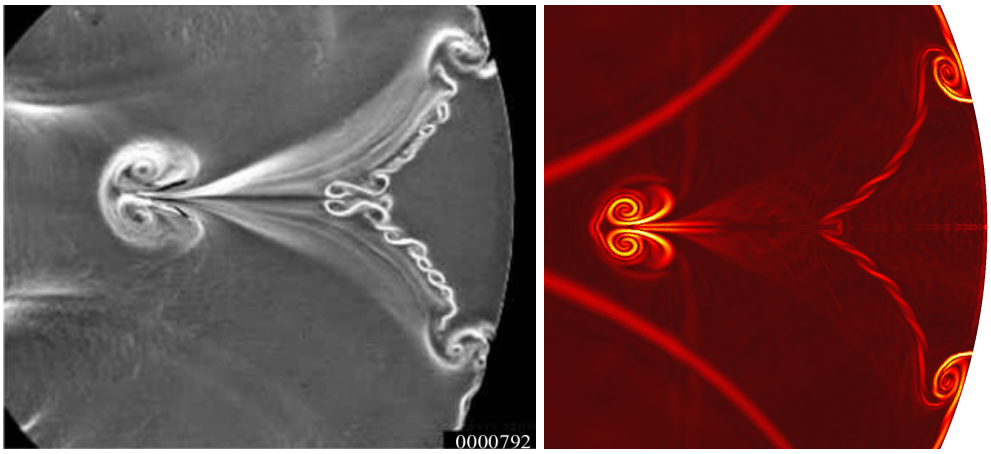

Figure 10: Experimental and simulation of the shock after hitting the cavity with the MOOD-$\mathbb{P}_3$ method. We observe that the structures are very well reproduced.

two other methods. In particular, the control of the polynomial degree is more efficient, the detection procedure faster and the physical restrictions of the solution are better included in the non-linear procedure. The capacity to handle unstructured meshes with different kind of cells and shapes associated to the low sensitivity to the form factor make the MOOD method a very versatile technology that, we expect, will be adopted in the next 10 years by a larger community.

ACKNOWLEDGEMENTS

This research was financed by FEDER Funds through Programa Operational Fatores de Competitividade — COMPETE and by Portuguese Funds FCT — Fundação para a Ciência e a Tecnologia, within the Projects PEst-C/MAT/UI0013/2014, PTDC/MAT/121185/2010 and FCT-ANR/MAT-NAN/0122/2012.

REFERENCES

[1] Dauxois, T, Peyrard, M., Ruffo, S. "The Fermi-Pasta-Ulam 'numerical experiment': history and pedagogical perspectives" Eur. J. Phys. Vol. **26** pp. 3-13, 2005.

[2] Von Neumann, R. D. Richtmyer, "A Method for the Numerical Calculation of Hydrodynamic Shocks. Journal of Applied Physics", Vol. **21**(3), pp. 232-237 (1950).

[3] Richtmyer R. D. and Morton K. W. "Difference Methods for Initial-Value Problems", second edition, Wiley-Interscience (1967).

[4] Godunov, S. K., "A Difference Scheme for Numerical Solution of Discontinuous Solution of Hydrodynamic Equations", Math. Sbornik, Vol. **47**, pp. 271-306, 1959.

[5] van Leer, B. , Towards the Ultimate Conservative Difference Scheme, V. A Second Order Sequel to Godunov's Method, J. Com. Phys., Vol. **32**, pp. 101-136, 1979.

[6] Buffard, T. , Clain, S., "Monoslope and multislope MUSCL methods for unstructured meshes", *J. Comput. Phys.* Vol. **229**, pp. 3745-3776, 2010.

[7] Casper J., Atkins, H. L., "A Finite-Volume High-Order ENO Scheme for Two-Dimensional Hyperbolic Systems", Journal of Computational Physics, Vol. **106**(1), pp. 62-76, 1993.

[8] Shu C.-W., "High order weighted essentially non-oscillatory schemes for convection dominated problems", SIAM Review, Vol. **51** pp. 82-126, 2009.

[9] Clain, S., Diot, S., Loubère, R., "A high-order finite volume method for hyperbolic systems: Multi-dimensional Optimal Order Detection (MOOD)", *J. Comput. Phys.* Vol. **230(10)**, pp. 4028-4050, 2011.

[10] Diot, S., Clain, S., Loubère, R., "Improved Detection criteria for the Multi-dimensional Optimal Order Detection (MOOD) on unstructured meshes with very high-order polynomials", *Comput. & Fluids* Vol. **64**, pp. 43-63, 2012.

[11] Clain, S., Figueiredo, J., "The MOOD method for the non-conservative shallow water system", preprint HAL hal-01077557 (2014), submitted.

[12] Diot, S., Loubère, R., Clain, S., "The MOOD method in the three-dimensional case: Very high-order finite volume method for hyperbolic systems", *Int. J. Numer. Meth. Fluids* Vol. **73**, pp. 362-392, 2013.

[13] S. Clain, G. Machado, J. M. Nóbrega, R. Pereira, A sixth-order finite volume method for multidomain convection-diffusion problem with discontinuous coefficients, Computer Methods in Applied Mechanics and Engineering, 267 (2013) 43–64.

[14] Toro, E. F., *Riemann Solvers and Numerical Methods for Fluid Dynamics*, 3^{rd} revision, Springer-Verlag Berlin and Heidelberg GmbH & Co. K 2009.

[15] Berthon, C., Desveaux, V., "An entropy preserving MOOD scheme for the Euler equations", *Int. J. finite volumes* Vol. **11**, pp. 1-39, 2014.

[16] S. Diot1, M.M. François, E.D. Dendy, A higher-order unsplit 2D direct Eulerian finite volume method for two-material compressible flows based on the MOOD paradigms, Int. J. Numer. Meth. Fluids (2014), Vol. **76**(12), pp. 1064-1087, 2014.

[17] M. Dumber, O. Zanotti, R. Loubère, S. Diot, A posteriori subcell limiting for discontinuous Galerkin finite element method for hyperbolic system of conservation laws, J. Comput. Phys. 278 (2014) 47–75.

[18] R. Loubère, M. Dumbser, S. Diot, A new family of high order unstructured MOOD and ADER finite volume schemes for multidimensional systems of hyperbolic conservation laws, Communications in Computational Physics 16 (2014) 718–763.

[19] Clain, S., Figueiredo, J., Second-order finite volume mood method for the shallow water with dry/wet interface, proceeding of the SYMCOMP2015, Faro, March 26-27, 2015, ECCOMAS, Portugal

[20] I.K. Nikolos, A.I. Delis, An unstructured node-centered finite volume scheme for shallow water flows with wet/dry fronts over complex topography, Comput. Methods Appl. Mech. Engrg. 198 (2009) 3723–3750.

[21] Skews B.W., Kleine H. Flow features resulting from shock wave impact on a cylindrical cavity. J. Fluid Mech Vol. **580** pp.481-93, 2007.